Published in final edited form as:
J Cell Sci. 2013 May 1; 126(0 9): 1981–1991. doi:10.1242/jcs.118315.

A complex containing LPP and α-Actinin mediates TGFβ-induced migration and invasion of ErbB2-expressing breast cancer cells

Elaine Ngan[1,2], **Jason J. Northey**[1,3], **Claire M. Brown**[5], **Josie Ursini-Siegel**[6], and **Peter M. Siegel**[*,1,2,3,4]

[1]Goodman Cancer Research Centre, McGill University, Montréal, Québec, Canada

[2]Department of Medicine, McGill University, Montréal, Québec, Canada

[3]Department of Biochemistry, McGill University, Montréal, Québec, Canada

[4]Department of Anatomy and Cell Biology, McGill University, Montréal, Québec, Canada

[5]Department of Physiology, McGill University, Montréal, Québec, Canada

[6]Lady Davis Institute for Medical Research, Montréal, Québec, Canada

Summary

Transforming Growth Factor β is a potent modifier of the malignant phenotype in ErbB2-expressing breast cancers. We demonstrate that epithelial-derived breast cancer cells, which undergo a TGFβ-induced EMT, engage signaling molecules that normally facilitate cellular migration and invasion of mesenchymal cells. We identify Lipoma Preferred Partner (LPP) as an indispensable regulator of TGFβ-induced migration and invasion of ErbB2-expressing breast cancer cells. We show that LPP re-localizes to focal adhesion complexes upon TGFβ stimulation and is a critical determinant in TGFβ-mediated focal adhesion turnover. Finally, we have determined that the interaction between LPP and α-Actinin, an actin cross-linking protein, is necessary for TGFβ-induced migration and invasion of ErbB2-expressing breast cancer cells. Thus, our data reveals that LPP, which is normally operative in cells of mesenchymal origin, can be co-opted by breast cancer cells during an EMT to promote their migration and invasion.

Keywords

breast cancer; ErbB2; TGFβ; EMT; LPP; migration; invasion

Introduction

Transforming Growth Factor β (TGFβ) promotes breast cancer cell metastasis to multiple sites, including the bone and lungs (Deckers et al., 2006; Kang et al., 2005; Mourskaia et al., 2009; Muraoka et al., 2003; Muraoka-Cook et al., 2004; Padua et al., 2008; Safina et al., 2011; Siegel et al., 2003; Yin et al., 1999). During breast cancer progression, TGFβ signaling enhances cell migration and invasion by modulating the expression and/or secretion of extracellular matrix components, proteases and adhesion molecules (Barcellos-Hoff and Akhurst, 2009; Padua and Massague, 2009; Safina et al., 2008; Wiercinska et al., 2011). While TGFβ is not itself oncogenic, cell-based and animal models have demonstrated

[*]Corresponding author: Peter M. Siegel, 1160 Pine Avenue West, Room 513, Montreal, Quebec, Canada, H3A 1A3 (514) 398-4259 (514) 398-6769peter.siegel@mcgill.ca.

Europe PMC Funders Author Manuscripts

its role in enhancing the aggressiveness of late-stage breast tumors (Barcellos-Hoff and Akhurst, 2009; Bierie and Moses, 2009; Derynck et al., 2001; Padua and Massague, 2009). Recently, TGFβ has been shown to modulate the mode by which breast cancer cells migrate and invade, with high levels of TGFβ signaling associated with single cell motility and blockade of this pathway resulting in cohesive breast cancer migration (Giampieri et al., 2009).

The cooperation between TGFβ and ErbB2 signaling pathways has been investigated in multiple cell-based models. These studies demonstrate that TGFβ can modulate the actin cytoskeleton and enhance cell migration of ErbB2 overexpressing breast cancer cells (Northey et al., 2008; Seton-Rogers et al., 2004; Ueda et al., 2004; Wang et al., 2006; Wang et al., 2008; Wang et al., 2009). Furthermore, studies in transgenic mouse models have shown that TGFβ can promote the formation of lung metastases by ErbB2-expressing mammary tumors (Muraoka et al., 2003; Siegel et al., 2003). Expression of a soluble ligand trap composed of the extracellular domain of the TGFβ type II receptor fused to the Fc portion of human IgG (Fc:TBRII) impedes the ability of ErbB2 induced mammary tumors to metastasize to the lung (Muraoka et al., 2002). Together, these data re-enforce the importance of interactions between the TGFβ and ErbB2 pathways in promoting breast cancer metastasis (Chow et al., 2011).

While TGFβ exerts an anti-proliferative effect on normal mammary epithelial cells and acts as a tumor suppressor, TGFβ can induce certain breast cancer cells to undergo an epithelial-to-mesenchymal transition (EMT) and promote tumor cell viability and migration (Derynck et al., 2001; Galliher and Schiemann, 2006; Muraoka et al., 2002; Rahimi and Leof, 2007; Safina et al., 2009; Wendt et al., 2010). TGFβ induces an EMT in epithelial cells, in part, through its ability to induce degradation of Par6 and disrupt tight-junctional complexes to enhance cell migration and metastasis (Ozdamar et al., 2005; Viloria-Petit et al., 2009). In addition, TGFβ signaling initiates a transcriptional program, involving Snail and Slug, which involves the upregulation of mesenchymal markers and the simultaneous repression of epithelial markers (Moustakas and Heldin, 2007; Xu et al., 2009). Through an EMT, breast tumor derived cells acquire new morphological changes and gene expression patterns characteristic of the mesenchymal lineage, which promote their migration, intravasation and extravasation and ultimately enhances the ability of breast cancer cells to metastasize (Hardy et al., 2010). Furthermore, breast cancers that exhibit features of an EMT acquire stem cell-like characteristics, are highly aggressive, are resistant to therapy, and are refractory to tumor suppressive processes such as apoptosis and senescence (Ansieau et al., 2008; Mani et al., 2008; Thiery et al., 2009; Tomaskovic-Crook et al., 2009). Another interesting consequence of an EMT stems from observations that TGFβ signaling responses are cell type dependent and as such, TGFβ can engage effectors in mesenchymal cells that are otherwise not involved in epithelial cell physiology (Alabert et al., 2006; Wilkes and Leof, 2006). Thus, an EMT may result in unique signaling pathways that can be engaged by TGFβ to promote breast cancer migration and invasion.

Lipoma Preferred Partner (LPP) belongs to the Zyxin family of LIM domain proteins, whose family members mediate cell migration, actin cytoskeletal remodeling and tumorigenesis (Hirota et al., 2000; Pratt et al., 2005; Willier et al., 2011; Yi and Beckerle, 1998). Studies of LPP in Smooth Muscle Cells (SMC), where it is highly expressed, have demonstrated its role in promoting cell migration, adhesion and the formation of lamellipodial extensions (Gorenne et al., 2003; Grunewald et al., 2009; Jin et al., 2007; Majesky, 2006; Petit et al., 2003; Vervenne et al., 2008). Overexpression of LPP enhances EGF-stimulated migration of vascular SMCs, whereas LPP-null mouse embryonic fibroblasts (MEF) exhibit reduced cell migration, further highlighting LPP's participation in regulating cell motility (Gorenne et al., 2003; Vervenne et al., 2009). LPP interacts with numerous proteins that are localized to cell-

cell contacts and focal adhesions, such as α-Actinin, Vasodilator-Stimulated Phosphoprotein (VASP), Scrib, Palladin and LIM and SH3 domain protein 1 (LASP-1), all of which function to modulate the actin cytoskeleton and have been implicated in human cancers (Grunewald et al., 2009; Jin et al., 2007; Keicher et al., 2004; Li et al., 2003; Petit et al., 2005; Vervenne et al., 2008; Zhang et al., 2009). Nonetheless, the role of LPP in promoting breast cancer metastasis has yet to be elucidated. In this study, we demonstrate that LPP is required for TGFβ-induced cell migration, cell invasion and focal adhesion turnover in ErbB2-expressing mammary tumor cells that undergo an EMT in response to TGFβ.

Results

LPP is required for TGFβ-induced migration and invasion of ErbB2-expressing cells that undergo an EMT

Previous studies have demonstrated that LPP enhances the migratory characteristics of mesenchymal cells (Gorenne et al., 2006; Gorenne et al., 2003; Jin et al., 2007). We have shown that ErbB2-transformed breast cancer cells (NMuMG-ErbB2) exhibit enhanced TGFβ-induced migration and invasion, concomitant with their ability to undergo an epithelial-to-mesenchymal transition (EMT) (Northey et al., 2008). Therefore, we reasoned that LPP may contribute to the migratory phenotype of these cells during the EMT process. To test this, we transiently reduced LPP levels in NMuMG-ErbB2 cells using siRNAs. In agreement with our previous results (Northey et al., 2008), TGFβ treatment induced a 2.5-fold average increase in the migration and a 2.6-fold average increase in the invasion of three independent NMuMG-ErbB2 tumor cells explants that were transfected with control siRNAs (Fig. 1A,B). In contrast, diminished LPP expression ablated TGFβ-induced migration and invasion in all three NMuMG-ErbB2 explant populations (Fig. 1A,B). Immunoblot analysis confirmed a significant reduction in LPP levels in cells transfected with LPP-targeting siRNAs compared to cells transfected with control siRNAs (Fig. 1C).

To interrogate a more general role for LPP in mediating TGFβ responses within ErbB2-expressing breast cancer cells, we first analyzed the human HER2-positive HCC1954 breast cancer cell line. Transient knockdown of LPP was sufficient to ablate the TGFβ-induced increase in migration (Fig. 1D) and invasion (Fig. 1E) seen in HCC1954 cells transfected with control siRNAs. Immunoblot analyses revealed endogenous LPP levels in control siRNA-transfected cells, which were efficiently reduced with LPP-targeting siRNAs (Fig. 1F). HCC1954 cells acquire mesenchymal marker expression (Fibronectin, α-SMA and Vimentin) following TGFβ stimulation (supplementary material Fig. S1A). However, we did not observe loss of E-cadherin expression in response to TGFβ. These cells are not growth inhibited by TGFβ (supplementary material Fig. S1B), but are responsive to TGFβ signaling as demonstrated by Smad2 phosphorylation (supplementary material Fig. S1C). These results were further extended by investigating the requirement of LPP in mediating the migration and invasion of an additional murine breast cancer cell line. Transfection of LPP siRNA into breast cancer cells explanted from MMTV/NIC (Neu/ErbB2-IRES-Cre) transgenic mice (Ursini-Siegel et al., 2008) abrogated TGFβ-induced cell migration and invasion (supplementary material Fig. S2A,B). Immunoblot analyses of cell lysates derived from NIC cells revealed a clear reduction in LPP levels by siRNA-mediated knockdown (supplementary material Fig. S2C). NIC cells undergo an EMT, as demonstrated by the loss of epithelial marker E-cadherin and the gain of mesenchymal markers (Vimentin and Fibronectin) in response to TGFβ stimulation (supplementary material Fig. S2D). Finally, NIC cells were modestly growth inhibited following TGFβ treatment (supplementary material Fig. S2E) and exhibited increased Smad2 phosphorylation in response to this cytokine (supplementary material Fig. S2F). Together, these data support an important role for LPP in enhancing the TGFβ-induced migration and invasion in both mouse and human ErbB2-expressing breast cancer models that undergo TGFβ-mediated EMT.

In contrast, TGFβ-stimulated migration of ErbB2-positive human SKBr3 breast cancer cells is independent of LPP (supplementary material Fig. S3A,B). SKBr3 cells are non-invasive, either in the basal state or following TGFβ stimulation, precluding us from examining a role for LPP in this context (data not shown). Interestingly, SKBr3 cells do not undergo a TGFβ stimulated EMT as assessed by comparable expression levels of epithelial markers (Claudin-3, Occludin) and mesenchymal markers (Snail, Vimentin) before and after TGFβ treatment (supplementary material Fig. S3C). SKBr3 cells harbor a deletion of E-Cadherin (Pierceall et al., 1995), which precludes assessment of this epithelial marker in response to TGFβ stimulation. TGFβ failed to induce a growth arrest response in SKBr3 cells (supplementary material Fig. S3D). Despite these negative results, TGFβ stimulation of these cells resulted in Smad2 phosphorylation, revealing that SKBr3 cells are indeed responsive to TGFβ treatment (supplementary material Fig. S3E). These data indicate that LPP-mediated migration and invasion of breast cancer cells requires increased cellular plasticity and the acquisition of a mesenchymal phenotype in response to TGFβ.

TGFβ induces LPP localization to focal adhesions in breast cancer cells, which requires signaling from the ErbB2 receptor

LPP is known to localize to focal adhesions in smooth muscle cells where it promotes the migratory properties of these mesenchymally-derived cells (Gorenne et al., 2003; Grunewald et al., 2009; Majesky, 2006; Petit et al., 2003; Vervenne et al., 2008). Therefore, we examined the sub-cellular localization of LPP in breast tumor explants expressing activated ErbB2 [NMuMG-ErbB2(NT)] or an attenuated ErbB2 receptor, which lacks the C-terminal autophosphorylation sites [NMuMG-ErbB2(NYPD)]. Our previous work has demonstrated that the C-terminal autophosphorylation sites of ErbB2 are required for TGFβ to increase breast cancer cell migration and invasion (Northey et al., 2008). Interestingly, following TGFβ treatment, LPP localization increased to include approximately 95% of vinculin-positive focal adhesions in NMuMG-ErbB2(NT) cells (Fig. 2A; Table 1). In contrast, LPP localization to vinculin-positive focal adhesions decreased (both percentage colocalization and staining intensity) in TGFβ-stimulated NMuMG-ErbB2(NYPD) cells (Fig. 2B; Table 1). Moreover, TGFβ stimulation also resulted in the localization of LPP to focal adhesions in the HCC1954 (Fig. 2C; Table 1) and NIC (data not shown) breast cancer cell models, which correlates with the ability of TGFβ to enhance the migratory and invasive phenotypes of these cells. The requirement of ErbB2-mediated signaling for TGFβ-induced localization to focal adhesions is reinforced by the observation that LPP fails to relocalize to focal adhesions following TGFβ treatment of parental NMuMG cells that lack ErbB2 expression (supplementary material Fig. S4). These data suggest that increased localization of LPP to focal adhesions following TGFβ treatment requires proper signaling downstream of ErbB2 and contributes to TGFβ-induced increases in migration and invasion.

Focal Adhesion targeting of LPP is required for TGFβ-induced migration and invasion of ErbB2-expressing breast cancer cells

We next established an inducible knockdown system using shRNAs targeting the 3′ untranslated region (UTR) of LPP. In this way, we are able to diminish the expression of endogenous LPP and re-express versions of LPP that allow us to define the functional domains of LPP that contribute to these processes. In complete agreement with our siRNA results (Fig. 1), we were able to show that doxycycline-induced knockdown of LPP, using two independent shRNAs, resulted in the complete loss of TGFβ-induced migration (supplementary material Fig. S5A) and invasion (supplementary material Fig. S5B) compared to cells that were not treated with doxycycline or those harboring a control shRNA. Immunoblot analysis confirmed doxycycline inducible knockdowns of LPP with both independent shRNAs and that ErbB2 levels remained similar in all of the cells, regardless of the LPP expression status (supplementary material Fig. S5C).

With this system in place, we next asked whether the focal adhesion targeting ability of LPP was required for its ability to promote TGFβ-induced migration and invasion of ErbB2-expressing breast cancer cells. To accomplish this, we generated an EGFP fusion protein with either wild-type LPP (LPP-WT) or a mutant form of LPP that harbors mutations in the first LIM domain (LPP-mLIM1) (Fig. 3A). Previous studies have shown that mutations engineered into the LIM domains of LPP abrogate the ability of this protein to target to focal adhesions (Petit et al., 2003). Immunoblot analysis revealed that endogenous LPP was efficiently reduced in cells following doxycycline treatment and expression of the EGFP-LPP-WT and EGFP-LPP-mLIM1 proteins was readily detected in cells as a slower migrating species, due to the GFP fusion (Fig. 3B). Expression of the EGFP-LPP fusion proteins was confirmed using antibodies against either the GFP or the LPP portion of the fusion protein. Finally, the ErbB2 levels remained uniform across the panel of NMuMG-ErbB2 cells (Fig. 3B). As expected, knockdown of endogenous LPP (VC) resulted in the complete ablation of TGFβ-induced migration (Fig. 3C) and invasion (Fig. 3D). Expression of the EGFP-LPP(WT) fusion protein, but not the EGFP-LPP-mLIM1 mutant, rescued the migration and invasion of NMuMG-ErbB2 cells in response to TGFβ treatment (Fig. 3C,D).

To ensure that the observed effects on migration and invasion that result from LPP loss were not secondary to other TGFβ-induced responses, we examined proliferation and induction of an EMT in response to TGFβ. We observed no differences in proliferation (supplementary material Fig. S6A), induction of Smad2 phosphorylation (supplementary material Fig. S6B) or an EMT (supplementary material Fig. S6C) in response to TGFβ treatment. Moreover, we confirmed that an intact Lim1 domain in LPP is required for localization to Vinculin-positive focal adhesions following TGFβ stimulation (supplementary material Fig. S7A,B). Together, these results indicate that the ability of LPP to promote enhanced migration and invasion of ErbB2-expressing cells in response to TGFβ requires its proper localization to focal adhesions.

LPP functions to promote focal adhesion turnover downstream of ErbB2 and TGFβ signaling

We previously demonstrated that co-activation of ErbB2(NT) and TGFβ signaling pathways results in the formation of smaller and more numerous focal adhesions, whereas breast cancer cells expressing a signaling defective ErbB2 receptor (NYPD) possessed fewer and larger focal adhesions (Northey et al., 2008). We hypothesize that TGFβ and ErbB2 signaling cooperate to enhance focal adhesion turnover and enhanced migration and invasion. To test this, we transfected cells with Paxillin-GFP to label focal adhesion complexes and employed fluorescence recovery after photo-bleaching (FRAP) to quantitatively assess the kinetics of focal adhesion turnover. High fluorescence recovery after photo-bleaching is indicative of dynamic focal adhesions that are being rapidly turned over. We demonstrate that 60% of the fluorescent signal was recovered after 60s following laser ablation in ErbB2(NT) cells under basal conditions, which increased significantly to 91% following TGFβ stimulation (Fig. 4A). In contrast, 79% fluorescence recovery was observed after 60s in ErbB2(NYPD) cells in the absence of TGFβ, which was reduced to 71% recovery following addition of TGFβ (Fig. 4A). When the $T_{1/2}$ measurements (time that 50% of fluorescent signal is recovered) were examined, ErbB2(NT) cells exhibited a $T_{1/2}$ = 45.4s in the absence of TGFβ, which decreased to $T_{1/2}$ = 20.8s following TGFβ treatment. In contrast, ErbB2(NYPD) expressing cells exhibited a $T_{1/2}$ = 22.4s without TGFβ treatment, which increased to $T_{1/2}$ = 37.8s following stimulation with TGFβ.

We further demonstrate that LPP is important for TGFβ-induced focal adhesion turnover. ErbB2(NT) cells retaining endogenous LPP expression (− Dox) exhibited 50% fluorescence recovery after 60s in the absence of TGFβ stimulation, which increased to 99% following addition of TGFβ (Fig. 4B). In contrast, reduced LPP levels (+ Dox) in ErbB2(NT) cells

underwent a similar rate of fluorescence recovery (65-70%) irrespective of TGFβ signaling (Fig. 4B). An examination of the $T_{1/2}$ values revealed that the presence of LPP was required for TGFβ to reduce the $T_{1/2}$ = 37.7s (− Dox, −β) to $T_{1/2}$ = 17.8s (− Dox, +β) in ErbB2(NT) expressing cells. In contrast, no TGFβ induced decreases in the $T_{1/2}$ were observed when endogenous LPP levels were reduced following doxycycline treatment of ErbB2(NT) cells (+ Dox, − β: $T_{1/2}$ = 22.2s; + Dox, + β: $T_{1/2}$ = 22.2s). These data support a role for LPP in promoting focal adhesion turnover downstream of the ErbB2 and TGFβ pathways.

α-Actinin fails to localize to stress fibers in cells that lack focal adhesion localized LPP

LPP is known to interact with numerous focal adhesion associated proteins, including Palladin, LASP1, Scrib and α-Actinin (Grunewald et al., 2009). We first examined whether TGFβ treatment of ErbB2(NT) or ErbB2(NYPD) cells revealed any differences in protein expression that might point to the particular importance of one of these LPP binding partners. Immunoblot analyses revealed that Palladin expression is very low in both ErbB2(NT) and ErbB2(NYPD) cells in the absence of TGFβ and is robustly up-regulated following TGFβ stimulation in both cell types (supplementary material Fig. S8A). In contrast, LASP1 and Scrib are uniformly expressed in both cell populations regardless of TGFβ engagement (supplementary material Fig. S8A). Finally, α-Actinin is also modestly induced following TGFβ treatment in both ErbB2(NT) and ErbB2(NYPD) cells (supplementary material Fig. S8A); however, to a much lesser extent than Palladin. Together, these results fail to reveal differences in the expression of LPP interacting partners that might explain the observed phenotypes.

We next examined the localization of LPP interacting partners in both ErbB2(NT) cells and ErbB2(NYPD) cells. We failed to see any differences in the TGFβ-induced localization of Palladin, Scrib or LASP1 in ErbB2(NT) versus ErbB2(NYPD) cells (supplementary material Fig. S8B). In contrast, we demonstrate that α-Actinin is localized to the cell periphery in untreated ErbB2(NT) cells and re-localizes to stress fibers upon TGFβ stimulation. While α-Actinin also localizes to the cell periphery in ErbB2(NYPD) cells, it fails to localize to stress fibers following TGFβ addition (supplementary material Fig. S9).

To conclusively link α-Actinin redistribution to LPP, we examined the localization of α-Actinin in ErbB2(NT) cells with or without LPP. As expected, α-Actinin moved from the cell periphery to stress fibers following TGFβ stimulation in cells retaining endogenous LPP (VC, −Dox). However, reduced LPP expression (VC, + Dox) impaired α-Actinin re-localization to stress fibers (Fig. 5A). To further correlate α-Actinin redistribution to the ability of LPP to localize to focal adhesions, we employed the EGFP-LPP-mLIM1 mutant that is defective in focal adhesion targeting. We first demonstrated that wild-type LPP (EGFP-LPP-WT) is sufficient to restore re-localization of α-Actinin from the cell periphery to stress fibers ErbB2(NT) cells in which endogenous LPP was reduced (Fig. 5B). In contrast, rescue with the EGFP-LPP-mLIM1 mutant, which cannot target to focal adhesions, fails to localize α-Actinin to stress fibers (Fig. 5C).

α-Actinin is the critical LPP binding partner involved in TGFβ-induced migration and invasion of ErbB2-expressing breast cancer cells

The α-Actinin binding domain within LPP has previously been defined (Li et al., 2003; Petit et al., 2003) (Fig. 6A). To specifically assess the role of α-Actinin in mediating LPP-induced migration and invasion downstream of TGFβ and ErbB2, we generated a mutant of LPP that cannot bind α-Actinin (LPP-ΔABD). We confirmed that, in the context of endogenous LPP knockdown, we could express similar levels of both the EGFP-LPP(WT) and EGFP-LPP(ΔABD) fusion proteins using both LPP and GFP-specific antibodies (Fig. 6B). Importantly, ErbB2 levels remained unchanged in any of the engineered cell

populations (Fig. 6B). We demonstrate that an intact α-Actinin binding domain is required for LPP to rescue TGFβ-induced migration (Fig. 6C) and invasion (Fig. 6D) of breast cancer cells with diminished levels of endogenous LPP. Co-immunoprecipitation experiments using anti-GFP antibodies confirmed that the EGFP-LPP(ΔABD) mutant was impaired in its ability to associate with α-Actinin relative to EGFP-LPP(WT) (supplementary material Fig. S10A).

We next asked whether the inability of LPP to interact with α-Actinin would affect LPP targeting to focal adhesions. Using the EGFP-LPP(WT) and EGFP-LPP(ΔABD) fusion proteins, we demonstrate that that LPP does not require α-Actinin to localize to focal adhesions (Fig. S10B). However, the ability of α-Actinin to redistribute from the cell periphery to stress fibers requires an intact α-Actinin binding domain in LPP (Fig. 7).

To ensure that the phenotypes we have observed with the EGFP-LPP(ΔABD) mutant are not secondary to alterations in other TGFβ responses, we compared TGFβ effects on proliferation, Smad2 phosphorylation and EMT in cells lacking LPP and those expressing LPP(WT) or LPP(ΔABD). We observed no differences in the doubling times for these cells in response to TGFβ treatment (supplementary material Fig. S11A) and detected the same degree of TFGβ-induced Smad2 phosphorylation in all populations (supplementary material Fig. S11B). Finally, loss of LPP or expression of LPP(ΔABD) had no adverse effects on the ability of TGFβ to induce an EMT in ErbB2(NT) breast cancer cells (supplementary material Fig. S11C). Taken together, these data demonstrate that the ability of LPP to promote TGFβ-induced migration and invasion requires its interaction with α-Actinin at focal adhesions.

Discussion

Numerous cell-based and transgenic mouse models demonstrate that ErbB2 and TGFβ signaling cooperatively promote breast cancer cell aggressiveness (Muraoka et al., 2002; Muraoka et al., 2003; Northey et al., 2008; Seton-Rogers et al., 2004; Siegel et al., 2003; Ueda et al., 2004; Wang et al., 2006; Wang et al., 2008; Wang et al., 2009). Nonetheless, the mechanisms underlying the synergy between these two pathways remain unclear. In the present study, we demonstrate using both transient and stable knock-down approaches that LPP is indispensable for mediating the migratory and invasive abilities of ErbB2-expressing breast cancer cells in response to TGFβ. The requirement for LPP to promote these aggressive cellular behaviors may be associated with the ability of breast cancer cells to undergo TGFβ-induced EMT. This observation is in agreement with several studies that demonstrate a role for LPP in modulating cytoskeletal dynamics and promoting cell migration in fibroblasts or Smooth Muscle Cells, in which it is highly expressed (Gorenne et al., 2003; Grunewald et al., 2009; Jin et al., 2007; Majesky, 2006; Petit et al., 2003; Vervenne et al., 2009; Vervenne et al., 2008). Hence, our data argue that breast cancer cells, which possess the ability to transition from an epithelial to a mesenchymal-like phenotype, can engage mediators that normally modulate migration in cells of mesenchymal origin.

LPP has been characterized as a protein that can translocate from sites of cell adhesion into the nucleus (Grunewald et al., 2009; Petit et al., 2003). Once in the nucleus, LPP has been shown to act as a transcription factor through domains located in the LIM and proline rich regions of the protein (Petit et al., 2000; Petit et al., 2003). LPP has also been shown to act as a transcriptional co-activator of Ets family transcription factors, such as PEA3 and ER81 (Guo et al., 2006). In this context, it is possible that LPP can co-operate with PEA3 to enhance the expression of target genes that have been implicated in breast cancer progression, invasion and metastasis (Guo et al., 2006). Recently, it has been shown that an EMT results in the re-localization of LPP from sites of cell-cell contact to focal adhesions.

In response to extracellular regulated signals transmitted via signaling networks at the focal adhesion, LPP translocates to the nucleus to modulate ETV5 transcriptional activity (Colas et al., 2012). While our study confirms that LPP is re-localized to focal adhesions during an EMT, we failed to observe TGFβ-induced LPP nuclear localization in any of the breast cancer cell lines employed in this study. Thus, we believe that LPP primarily functions to regulate the actin cytoskeleton during focal adhesion formation, leading to increased cell migration.

LPP is uniquely positioned to regulate the actin cytoskeleton during cell migration due to its ability to target to focal adhesions (Petit et al., 2003). LPP augments the EGF-induced migration of vascular smooth muscle cells (Gorenne et al., 2003), whereas loss of LPP expression results in diminished fibroblast migration (Gorenne et al., 2006). Interestingly, we show that signaling initiated from the activated ErbB2 receptor is necessary for the re-localization of LPP to focal adhesions in response to TGFβ. The importance of LPP targeting to focal adhesions is evident from the fact that a LPP mutant, which can no longer target to focal adhesions, fails to rescue TGFβ-induced migration and invasion. Our study is the first to functionally implicate LPP as a mediator capable of enhancing the TGFβ-induced focal adhesion turnover of ErbB2 expressing mammary tumor cells.

LPP may exert its pro-migratory effects via its ability to bind α-Actinin (Hansen and Beckerle, 2008; Li et al., 2003). We demonstrate that loss of α-Actinin binding to LPP has the same effect as the complete loss of LPP, suggesting that α-Actinin is the major downstream mediator through which LPP functions to enhance the migration and invasion of ErbB2 expressing breast cancer cells in response to TGFβ. The role of α-Actinin in promoting cell migration, tumorigenesis and metastasis has been described in various human cancers, including breast cancer (Otey and Carpen, 2004; Sjoblom et al., 2008). Previous studies have argued for a role of α-Actinin at the leading edge of ErbB2-expressing breast cancer cells that were stimulated with TGFβ (Wang et al., 2006). However, our data suggests that in breast cancer cells undergoing a TGFβ-induced EMT, α-Actinin is localized to focal adhesions/stress fibers by LPP, which can then serve a critical role in regulating focal adhesion stability and turnover. Indeed, α-Actinin is a molecular scaffold that links actin filaments and focal adhesions (Vicente-Manzanares et al., 2009). Furthermore, knockdown of α-Actinin leads to the formation of stable adhesions (Choi et al., 2008), underscoring its role in regulating focal adhesion turnover and disassembly.

One mechanism by which α-Actinin can influence focal adhesion turnover involves the engagement of Calpains to destabilize focal adhesions, which in turn leads to their disassembly. Calpains are a family of proteases that have been shown to cleave proteins within adhesion complexes, such as: α-Actinin, Vinculin, FAK, Talin, β-containing Integrins and Paxillin (Franco and Huttenlocher, 2005). It has been shown that α-Actinin, which is localized along stress fibers, can interact directly with MEKK1 and subsequently modulate the activity of Calpain. Thus, an α-Actinin/MEKK1/Calpain pathway can be engaged that results in the disassembly of focal adhesion complexes, which can promote cell migration (Christerson et al., 1999; Cuevas et al., 2003; Franco and Huttenlocher, 2005; Otey and Carpen, 2004). Interestingly, it has been previously demonstrated that Calpain activity is required for the disassembly of Vinculin and Zyxin containing focal adhesions (Bhatt et al., 2002). Furthermore, inhibition of Calpains prevented localization of α-Actinin to focal adhesion sites and resulted in its accumulation at the cell periphery (Bhatt et al., 2002). Therefore, it is conceivable that TGFβ stimulation targets LPP to focal adhesions and promotes α-Actinin re-localization from the cell periphery to stress fibers, resulting in Calpain-mediated focal adhesion turnover. Whether MEKK1-mediated Calpain activation leads to subsequent focal adhesion turnover will require further investigation. This is plausible given previous studies that link TGFβ stimulation to MEKK1 in the process of cell

migration, cytoskeletal reorganization and tissue remodeling in both epithelial cells and fibroblasts (Liu et al., 2007; Zhang et al., 2003).

An exciting new concept is emerging, which argues that force-dependent mechanisms play a prominent role in modulating focal adhesion dynamics (Grashoff et al., 2010; Wolfenson et al., 2011). While focal adhesions are sites of contact between the cytoskeleton and the ECM, they also act as mechanosensors which respond to tensional changes to the microenvironment. Together, they convert chemical and mechanical stimuli into biological responses that alter cellular behavior. Several studies suggest potential roles for α-Actinin in mediating the cellular response to changes in extracellular matrix elasticity. Early in vitro studies of α-Actinin in 2D rafts of F-actin revealed that this protein does not simply fulfill the role of a rigid spacer between actin filaments, but rather could serve as a tension sensor between the ECM and the actin cytoskeleton (Hampton et al., 2007). Recent evidence is now emerging to support this hypothesis. Glioblastoma cells, which have reduced α-Actinin levels, exhibit diminished migration as a result of their inability to adapt to changes in the ECM elasticity and a failure to generate maximal cell-ECM tractional forces (Sen et al., 2009). In addition to the effects of actomyosin contractility forces on focal adhesion assembly and turnover, it has recently been demonstrated that the network of radial stress fibers, which relies on α-Actinin function, also controls focal adhesion maturation (Oakes et al., 2012).

Members of the Zyxin family are emerging as mediators of mechanotransduction, which can influence focal adhesion turnover in response to mechanical cues (Lele et al., 2006). While a role for LPP in modulating force-dependent cellular behavior is only just starting to be elucidated, many studies have shown that Zyxin is targeted to focal adhesions in a force-dependent manner (Hirata et al., 2008; Lele et al., 2006) Furthermore, the LIM domains of Zyxin are necessary and sufficient for its localization to adhesion complexes under these conditions (Uemura et al., 2011). Interestingly, we have shown that the LIM1 domain of LPP is indispensable for its focal adhesion targeting ability. We also show that LPP functions require the action of α-Actinin, which is heavily implicated in force-mediated focal adhesion maturation and disassembly as well. Hence, it is conceivable that LPP is recruited to force-bearing adhesional complexes through its LIM1 domain, which recruits α-Actinin as a mechanism to facilitate focal adhesion turnover and disassembly downstream of TGFβ and ErbB2 signaling.

Materials and methods

Cell culture

The NMuMG-derived cell populations and explants were maintained as previously described (Northey et al., 2008). When indicated, cells were treated with 1μg/mL doxycycline (Cat. #: D9891, Sigma-Aldrich) for 72 - 96 hours prior to further experimentation. The NIC cell line was established from a primary mammary tumor-derived from the MMTV/NIC transgenic mouse model (Ursini-Siegel et al., 2008) and maintained in DMEM supplemented with 5% FBS and 1× MEGS (Cat. #: S-015-5, Invitrogen). HCC1954 and SkBr3 cells were obtained from the American Type Culture Collection and maintained in RPMI supplemented with 10% FBS following ATCC guidelines. All cell populations were stimulated with 2ng/mL of TGF-β1 (Cat# HZ-1011, Humanzyme) for the indicated times.

Retroviral production was performed using Retro-X Universal Packaging System according to manufacturer's protocol (Cat. #: 631530, Clontech). NMuMG cells were then incubated with polybrene (8ug/mL), and a 50:50 mix of virus containing media/fresh cell media for 24 hours for retroviral infection.

Migration and Invasion Assays

NMuMG-derived cell populations and NIC cells, treated with or without TGFβ, were trypsinized and resuspended in serum-free media prior to plating into Boyden chambers. Migration and invasion assays were performed as previously described (Northey et al., 2008). To quantify the migration and invasion data, 5 images/well were acquired from each transwell using a camera-equipped microscope and the 10× objective. The pixel count for all images was obtained using Scion Image software (Scion Corporation). The data represents the average of 3 independent experiments performed in duplicate. NMuMG-ErbB2(NT) explants described in Figure 1, and NIC cells were plated at a density of 6×10^4 cells for the migration assays and 9×10^4 cells for the invasion assays. In all other experiments, 9×10^4 or 1.5×10^5 NMuMG cells were used for migration and invasion assays, respectively. HCC1954 and SkBr3 cell migration and invasion were assessed by plating 4×10^5 cells, resuspended in serum free media, into xCELLigence CIM plates (Cat. #: 05665825001, Roche Applied Science). The rates of cell migration and invasion were monitored for 24 hours in a RTCA DP Analyzer (Roche Applied Science) and calculated according to manufacturer's protocol using the xCELLigence RTCA software (Roche Applied Science). The data shown represents the average from 3 independent experiments performed in duplicate.

siRNA and shRNA-mediated LPP Knockdowns

The following siRNA sequences targeting mouse *LPP* were used: AGC-GCA-UAG-AGA-AUA-CGA-UU and AGA-AGA-CCU-AUA-UCA-CAG-AC. The following siRNA sequences targeting human *LPP* were used: GGA-AGA-UAG-UCU-UAU-GUA, CCC-AGU-UUA-AGA-CAC-CAA and GCC-AAG-UUA-AAU-AGC-AAA. Both mouse and human siRNAs were acquired from IDT (Cat. #: MMC.RNAI.N178665.8.1, MMC.RNAI.N178665.8.3, HSC.RNAI.N005578.12.1, HSC.RNAI.N005578.12.2, HSC.RNAI.N005578.12.3, Integrated DNA Technologies). Cells were transfected with a pool of 2 or 3 siRNAs, each at a concentration of 2nM, or a control non-targeting siRNA (AGU-UAA-UCG-CGU-AUA-AUA) using INTERFERrin transfection reagent (Cat. #: 409-50, Polyplus transfection) according to manufacturer's protocol. To confirm efficient LPP knockdown, total cell lysates were collected at the endpoint of each migration/invasion assay and immunoblotted for LPP.

To establish an inducible knockdown system for LPP, NMuMG parental cells were infected with a pMSCV-hygro viral vector harboring the rat orthologue of ErbB2, which possessed the activating transmembrane point mutation V664E (Bargmann and Weinberg, 1988). Cells were subsequently infected with the pRev-Tet-On retroviral vector (Cat. #: 631007, Clontech). The following shRNA sequences were expressed in the TMP vector system (Cat. #: EAV4678, Open Biosystems): L#1: TGC-TGT-TGA-CAG-TGA-GCG-CGC-GCA-TAG-AGA-ATA-CGA-TTT-GTA-GTG-AAG-CCA-CAG-ATG-TAC-AAA-TCG-TAT-TCT-CTA-TGC-GCT-TGC-CTA-CTG-CCT-CGG-A, L#2: TGC-TGT-TGA-CAG-TGA-GCG-AGG-AGA-CTG-TGT-GAA-AGA-GAA-ATA-GTG-AAG-CCA-CAG-ATG-TAT-TTC-TCT-TTC-ACA-CAG-TCT-CCC-TGC-CTA-CTG-CCT-CGG-A. Additionally, a shRNA sequence targeting Luciferase (TGC-TGT-TGA-CAG-TGA-GCG-CTG-ATT-ATG-TCC-GGT-TAT-GTA-ATA-GTG-AAG-CCA-CAG-ATG-TAT-TAC-ATA-ACC-GGA-CAT-AAT-CAT-TGC-CTA-CTG-CCT-CGG-A) was inserted into the TMP system and served as a negative control. Sequences were PCR amplified, digested and cloned into the TMP vector according to manufacturer's protocol. The sequences within the TMP vector encoding GFP were removed by restriction enzyme digestion and the resulting vectors were introduced into the cells via retroviral infection.

Immunoblotting and immunofluorescence

Cells were cultured to 80% confluency and lysed in ice cold TNE lysis buffer as previously described (Northey et al., 2008). Total cell lysates (20μg) were resolved by 6-12% SDS-PAGE. Proteins were transferred onto PVDF membranes (Cat. #: IPVH00010, Millipore) and membranes were blocked in 5% fat-free milk overnight. The following day, membranes were incubated with the respective primary antibodies for 1 hour: LPP (1:1000; Cat. #: 3389S, Cell Signaling), ErbB2 (1:200; Cat. #: SC-284, Santa Cruz), GFP (1:1000; Cat. #: AB3080, Millipore), E-cadherin (1:1000; Cat. #: U3254, Sigma), Fibronectin (1:5000; Cat. #: F3648, Sigma), Vimentin (1:1000; Cat. #: 550513, BD Biosciences), pSmad2 (1:1000; Cat. #: 3101, Cell Signaling), Smad2/3 (1:1000; Cat. #: 3102, Cell Signaling), Snail (1:1000; Cat. #: 3895, Cell Signaling), Claudin-3 (1:1000; Cat. #: 34-1700, Invitrogen), Occludin (1:1000; Cat. #: 71-1500, Invitrogen), α-SMA (1:1000; Cat. #: A2547, Sigma), Palladin (1:1000; Cat. #: 10853-1-AP, Proteintech), LASP1 (1:500; Cat. #: HPA012072, sigma), Scrib (1:1000; Cat. #: sc-11049, Santa Cruz), α-Actinin (1:1000; Cat. #: AB18061, Abcam) and α-Tubulin (1:40,000; Cat #: T9026, Sigma). The appropriate HRP-conjugated secondary antibodies (1:10,000; Jackson Immuno Research Laboratories) were incubated for 1 hour and the membranes were visualized using Pierce Enhanced Chemiluminescence (ECL) (Cat #: 32106, Thermo Scientific).

NMuMG derivatives and HCC1954 cells were plated onto glass coverslips in 24-well plates and allowed to grow to 70% confluency. Cells were then stimulated with or without TGFβ for the indicated amount of time. A scratch was made in the confluent cell monolayer using a blunted p200 pipette tip and cells were allowed to migrate into the wound for 6 hours. For immunofluorescence staining, media was removed from the wells and cells were fixed in 2% PFA for 20 minutes or with 4% PFA for 1 minute followed by ice cold Methanol for 10 minutes. Cells were then permeabilized with 0.2% triton X-100, rinsed with 100mM Glycine in PBS and blocked in 2% Bovine Serum Albumin in IF buffer (0.2% Triton X-100 and 0.05% Tween-20 in PBS). The following antibodies were incubated with the coverslips for 1 hour: LPP (1:500, Cat. #: SC-27312, Santa Cruz), Vinculin (1:750, Cat. #: V9131, Sigma-Aldrich), GFP (1:500, Cat. #: AB3080, Millipore), α-Actinin (1:500, Cat. #: AB18061, Abcam), Palladin (1:500; Cat. #: 10853-1-AP, Proteintech), LASP1 (1:200; Cat. #: HPA012072, Sigma), Scrib (1:500; Cat. #: sc-11049, Santa Cruz) and Alexa Fluor 488 Phalloidin (1:500; Cat. #: A12379, Invitrogen. The appropriate Alexa Fluor dye conjugated secondary antibodies were used (488nm or 555nm, Invitrogen) and DAPI (Cat. #: D3571, Invitrogen) was used to visualize the nucleus. Images were acquired along the wound in the cell monolayer. Image acquisition was performed with ZEN imaging software on a Zeiss LSM510/Axiovert 200M confocal microscope and a plan-Apochromat 63×/1.4 NA oil objective (Carl Zeiss Inc.).

Fluoresecence Recovery after Photo-bleaching (FRAP)

NMuMG-ErbB2 NT and NYPD cells were transfected with Paxillin-GFP (A gift from Dr. Rick Horwtiz, University of Virginia) using Effectene reagent (Cat. #: 301427, Qiagen). Cells were then plated onto glass bottom culture dishes coated with 5μg/cm^2 of fibronectin (Cat. #: FC010, Millipore), and stimulated with or without TGFβ for 24 hours. The cultured dishes were placed into a temperature and humidity controlled chamber attached to a Zeiss LSM510/Axiovert 200M confocal microscope (Carl Zeiss Inc.) for FRAP analysis. Cells were visualized with a plan-Apochromat 63×/1.4 NA oil objective and 1 to 5 adhesions at the leading edge of the cells, as marked by Paxillin-GFP, were photo-bleached using an argon laser for 15 cycles at full laser power. The fluorescence recovery was monitored for an additional 60 seconds. The raw fluorescence values collected were normalized against a non-bleached adhesion and expressed as a percentage of recovery. The normalized data was then fitted to an exponential recovery curve using ImageJ software (http://imagej.nih.gov/ij).

The % recovery at 60s for each sample is plotted and is representative of an average of 12-19 adhesions. The same procedure was used with NMuMG-ErbB2 cells expressing a LPP targeting shRNA, except cells were treated with or without doxycycline for 72 hours prior to plating onto glass bottom culture dishes coated with fibronectin and a total of 18-28 adhesions were analyzed per cell population.

Proliferation Assay

To complete proliferation assays, 1.5×10^4 HCC 1954 cells, 5×10^3 NMuMG-ErbB2 derived cells, 1×10^4 NIC tumor-derived cells and 2×10^4 SKBr3 cells were plated into xCELLigence E-plates (Cat. #: 05469813001, Roche Applied Science) and incubated in the presence or absence of TGFβ. Cell growth was monitored in a RTCA DP Analyzer (Roche Applied Science) for up to 96 hours and the doubling time was calculated using the xCELLigence RTCA software (Roche Applied Science) according to manufacturer's protocol.

Co-Immunoprecipitation

NMuMG-ErbB2 derived cells were incubated with or without doxycycline for 72 hours, in the presence or absence of TGFβ for 24 hours. Cells were cultured to 80% confluency and lysed in ice cold TNE lysis buffer. Protein lysates were quantified and 1mg of total protein was incubated overnight at 4°C in 500 uL of TNE lysis buffer containing an anti-GFP antibody (1:1000; Cat. #: A10260, Invitrogen) and 20uL of a 50% Protein G Sepharose bead slurry (Cat. #: 17-0618-02, GE Healthcare). Following incubation, sepharose beads were pelleted and washed four times in TNE lysis buffer and proteins were eluted with 2× SDS loading buffer (Tris/HCl, Glycerol, SDS and β-Mercaptoethanol). The supernatant was divided into three equal aliquots for SDS-PAGE.

Construction of LPP mutants

LPP cDNA was purchased from Open Biosystems as an insert in pCMV-SPORT6 vector (Cat #:MMM1013-98478393, Open Biosystems). Full length LPP was shuttled into *SphI/XhoI* sites of the pGEM7zf vector (cat #:P2251, Promega) as a *SalI/SphI* fragment. The vector was then enzymatically digested with *PshAI/ApaI* and the product was ligated into *Ecl136*II/*Apa*I of pEGFP-C1 vector (cat #: 6084-1, Clontech) to produce an EGFP-LPP fusion product. Then, EGFP-LPP was PCR amplified into *Sal*I/*Eco*RI sites of pMSCV vector (cat #: 634401, Clontech), modified to express a blasticidin resistance marker. To construct the EGFP-LPP-mLIM1 and EGFP-LPP-ΔABD mutants, QuikChange site directed mutagenesis kit (cat #: 210518, Stratagene) was used according to manufacturer's protocol and primers were designed using the QuikChange Primer Design Program (www.genomics.agilent.com). The EGFP-LPP constructs were retrovirally infected into NMuMG cells and maintained in 40g/mL of blasticidin (Cat #: BLA477.100, Bioshop Canada Inc.).

Quantification of LPP and Vinculin colocalization

To assess for colocalization, Vinculin adhesions were identified and isolated to create a binary object mask. The object mask was then used to identify and quantify LPP localization within Vinculin-positive adhesions. More specifically, immunofluorescence confocal images of LPP and Vinculin were exported from ZEN imaging software (Carl Zeiss Inc., Jena, Germany) into respective raw data single plane 8-bit TIF format images. To facilitate processing, images from channels representing LPP and Vinculin staining were then imported into MetaMorph image analysis software (Molecular Devices Inc., Sunnyvale, CA) and converted into 16-bit format. To permit accurate identification of Vinculin-containing adhesions, noise was removed from vinculin images using a median filter with a 5×5 pixel kernel. Thresholding was then applied to the filtered image to identify and isolate Vinculin-

positive focal adhesions, while excluding the surrounding cytoplasmic regions. Integrated Morphometry Analysis (IMA) was used to create a binary object mask of regions of interest corresponding to the adhesions. An area filter of > 20 pixels was applied to the identified regions in order to remove small spots corresponding to regions of nonspecific antibody staining or debris in the sample. The binary object mask was applied to the raw background corrected LPP and vinculin images and IMA was used to count the number and intensity of vinculin and LPP positive adhesions. Seven to fourteen sets of images containing at least one cell for each cell line were quantified. The total number of adhesions quantified for each cell line is as follows: NT −β = 1170, NT + β = 1440, NYPD − β = 1505, NYPD + β = 1625, HCC1954 − β = 2139, HCC1954 + β = 3671.

Statistical Analysis

Statistical significance values (*p* values) for migration and invasion assays were obtained by performing a two-sample unequal variance student's t-test.

Supplementary Material

Refer to Web version on PubMed Central for supplementary material.

Acknowledgments

We thank members of the Siegel laboratory for helpful discussions and their critical comments on the manuscript. We acknowledge support from Dr. Claire Brown and the McGill Life Science Complex Imaging facility for the FRAP analysis. E.N. was supported by a studentship from the Fonds de recherche en santé du Québec (FRSQ) and currently holds a studentship from the US Army Department of Defense Breast Cancer Research Program (W81XWH-11-1-0008), J.J.N. was supported by studentships from the Research Institute of the McGill University Health Centre and Department of Medicine, McGill University, J.U-S. holds a CIHR New Investigator Salary Support award and P.M.S. was a Research Scholar (Junior II) of the FRSQ. This work was supported by grants from the Association for International Cancer Research (AICR, 11-0204) and the Canadian Cancer Society (CCSRI, 2011-700790) to P.M.S. and a CIHR operating grant (MOP-111143) to J.U-S.

References

Alabert C, Rogers L, Kahn L, Niellez S, Fafet P, Cerulis S, Blanchard JM, Hipskind RA, Vignais ML. Cell type-dependent control of NF-Y activity by TGF-beta. Oncogene. 2006; 25:3387–96. [PubMed: 16434965]

Ansieau S, Bastid J, Doreau A, Morel AP, Bouchet BP, Thomas C, Fauvet F, Puisieux I, Doglioni C, Piccinin S, et al. Induction of EMT by twist proteins as a collateral effect of tumor-promoting inactivation of premature senescence. Cancer cell. 2008; 14:79–89. [PubMed: 18598946]

Barcellos-Hoff MH, Akhurst RJ. Transforming growth factor-beta in breast cancer: too much, too late. Breast cancer research: BCR. 2009; 11:202. [PubMed: 19291273]

Bargmann CI, Weinberg RA. Oncogenic activation of the neu-encoded receptor protein by point mutation and deletion. EMBO J. 1988; 7:2043–2052. [PubMed: 2901345]

Bhatt A, Kaverina I, Otey C, Huttenlocher A. Regulation of focal complex composition and disassembly by the calcium-dependent protease calpain. Journal of cell science. 2002; 115:3415–25. [PubMed: 12154072]

Bierie B, Moses HL. Gain or loss of TGFbeta signaling in mammary carcinoma cells can promote metastasis. Cell cycle. 2009; 8:3319–27. [PubMed: 19806012]

Choi CK, Vicente-Manzanares M, Zareno J, Whitmore LA, Mogilner A, Horwitz AR. Actin and alpha-actinin orchestrate the assembly and maturation of nascent adhesions in a myosin II motor-independent manner. Nature cell biology. 2008; 10:1039–50.

Chow A, Arteaga CL, Wang SE. When tumor suppressor TGFbeta meets the HER2 (ERBB2) oncogene. Journal of mammary gland biology and neoplasia. 2011; 16:81–8. [PubMed: 21590373]

Christerson LB, Vanderbilt CA, Cobb MH. MEKK1 interacts with alpha-actinin and localizes to stress fibers and focal adhesions. Cell motility and the cytoskeleton. 1999; 43:186–98. [PubMed: 10401575]

Colas E, Muinelo-Romay L, Alonso-Alconada L, Llaurado M, Monge M, Barbazan J, Gonzalez M, Schoumacher M, Pedrola N, Ertekin T, et al. ETV5 cooperates with LPP as a sensor of extracellular signals and promotes EMT in endometrial carcinomas. Oncogene. 2012

Cuevas BD, Abell AN, Witowsky JA, Yujiri T, Johnson NL, Kesavan K, Ware M, Jones PL, Weed SA, DeBiasi RL, et al. MEKK1 regulates calpain-dependent proteolysis of focal adhesion proteins for rear-end detachment of migrating fibroblasts. The EMBO journal. 2003; 22:3346–55. [PubMed: 12839996]

Deckers M, van Dinther M, Buijs J, Que I, Lowik C, van der Pluijm G, ten Dijke P. The tumor suppressor Smad4 is required for transforming growth factor beta-induced epithelial to mesenchymal transition and bone metastasis of breast cancer cells. Cancer research. 2006; 66:2202–9. [PubMed: 16489022]

Derynck R, Akhurst RJ, Balmain A. TGF-beta signaling in tumor suppression and cancer progression. Nature genetics. 2001; 29:117–29. [PubMed: 11586292]

Franco SJ, Huttenlocher A. Regulating cell migration: calpains make the cut. Journal of cell science. 2005; 118:3829–38. [PubMed: 16129881]

Galliher AJ, Schiemann WP. Beta3 integrin and Src facilitate transforming growth factor-beta mediated induction of epithelial-mesenchymal transition in mammary epithelial cells. Breast cancer research: BCR. 2006; 8:R42. [PubMed: 16859511]

Giampieri S, Manning C, Hooper S, Jones L, Hill CS, Sahai E. Localized and reversible TGFbeta signalling switches breast cancer cells from cohesive to single cell motility. Nature cell biology. 2009; 11:1287–96.

Gorenne I, Jin L, Yoshida T, Sanders JM, Sarembock IJ, Owens GK, Somlyo AP, Somlyo AV. LPP expression during in vitro smooth muscle differentiation and stent-induced vascular injury. Circ Res. 2006; 98:378–85. [PubMed: 16397143]

Gorenne I, Nakamoto RK, Phelps CP, Beckerle MC, Somlyo AV, Somlyo AP. LPP, a LIM protein highly expressed in smooth muscle. Am J Physiol Cell Physiol. 2003; 285:C674–685. [PubMed: 12760907]

Grashoff C, Hoffman BD, Brenner MD, Zhou R, Parsons M, Yang MT, McLean MA, Sligar SG, Chen CS, Ha T, et al. Measuring mechanical tension across vinculin reveals regulation of focal adhesion dynamics. Nature. 2010; 466:263–6. [PubMed: 20613844]

Grunewald TG, Pasedag SM, Butt E. Cell Adhesion and Transcriptional Activity - Defining the Role of the Novel Protooncogene LPP. Transl Oncol. 2009; 2:107–16. [PubMed: 19701494]

Guo B, Sallis RE, Greenall A, Petit MM, Jansen E, Young L, Van de Ven WJ, Sharrocks AD. The LIM domain protein LPP is a coactivator for the ETS domain transcription factor PEA3. Mol Cell Biol. 2006; 26:4529–38. [PubMed: 16738319]

Hampton CM, Taylor DW, Taylor KA. Novel structures for alpha-actinin:F-actin interactions and their implications for actin-membrane attachment and tension sensing in the cytoskeleton. Journal of molecular biology. 2007; 368:92–104. [PubMed: 17331538]

Hansen MD, Beckerle MC. alpha-Actinin links LPP, but not zyxin, to cadherin-based junctions. Biochemical and biophysical research communications. 2008; 371:144–8. [PubMed: 18413140]

Hardy KM, Booth BW, Hendrix MJ, Salomon DS, Strizzi L. ErbB/EGF signaling and EMT in mammary development and breast cancer. Journal of mammary gland biology and neoplasia. 2010; 15:191–9. [PubMed: 20369376]

Hirata H, Tatsumi H, Sokabe M. Zyxin emerges as a key player in the mechanotransduction at cell adhesive structures. Communicative & integrative biology. 2008; 1:192–195. [PubMed: 19513257]

Hirota T, Morisaki T, Nishiyama Y, Marumoto T, Tada K, Hara T, Masuko N, Inagaki M, Hatakeyama K, Saya H. Zyxin, a regulator of actin filament assembly, targets the mitotic apparatus by interacting with h-warts/LATS1 tumor suppressor. The Journal of cell biology. 2000; 149:1073–86. [PubMed: 10831611]

Jin L, Kern MJ, Otey CA, Wamhoff BR, Somlyo AV. Angiotensin II, focal adhesion kinase, and PRX1 enhance smooth muscle expression of lipoma preferred partner and its newly identified binding partner palladin to promote cell migration. Circ Res. 2007; 100:817–25. [PubMed: 17322171]

Kang Y, He W, Tulley S, Gupta GP, Serganova I, Chen CR, Manova-Todorova K, Blasberg R, Gerald WL, Massague J. Breast cancer bone metastasis mediated by the Smad tumor suppressor pathway. Proceedings of the National Academy of Sciences of the United States of America. 2005; 102:13909–14. [PubMed: 16172383]

Keicher C, Gambaryan S, Schulze E, Marcus K, Meyer HE, Butt E. Phosphorylation of mouse LASP-1 on threonine 156 by cAMP- and cGMP-dependent protein kinase. Biochem Biophys Res Commun. 2004; 324:308–16. [PubMed: 15465019]

Lele TP, Pendse J, Kumar S, Salanga M, Karavitis J, Ingber DE. Mechanical forces alter zyxin unbinding kinetics within focal adhesions of living cells. Journal of cellular physiology. 2006; 207:187–94. [PubMed: 16288479]

Li B, Zhuang L, Reinhard M, Trueb B. The lipoma preferred partner LPP interacts with {alpha}-actinin. J Cell Sci. 2003; 116:1359–1366. [PubMed: 12615977]

Liu S, Xu SW, Kennedy L, Pala D, Chen Y, Eastwood M, Carter DE, Black CM, Abraham DJ, Leask A. FAK is required for TGFbeta-induced JNK phosphorylation in fibroblasts: implications for acquisition of a matrix-remodeling phenotype. Molecular biology of the cell. 2007; 18:2169–78. [PubMed: 17409352]

Majesky MW. Organizing Motility: LIM Domains, LPP, and Smooth Muscle Migration. Circ Res. 2006; 98:306–308. [PubMed: 16484626]

Mani SA, Guo W, Liao MJ, Eaton EN, Ayyanan A, Zhou AY, Brooks M, Reinhard F, Zhang CC, Shipitsin M, et al. The epithelial-mesenchymal transition generates cells with properties of stem cells. Cell. 2008; 133:704–15. [PubMed: 18485877]

Mourskaia AA, Dong Z, Ng S, Banville M, Zwaagstra JC, O'Connor-McCourt MD, Siegel PM. Transforming growth factor-beta1 is the predominant isoform required for breast cancer cell outgrowth in bone. Oncogene. 2009; 28:1005–15. [PubMed: 19079339]

Moustakas A, Heldin CH. Signaling networks guiding epithelial-mesenchymal transitions during embryogenesis and cancer progression. Cancer science. 2007; 98:1512–20. [PubMed: 17645776]

Muraoka R, Dumont N, Ritter C, Dugger T, Brantley D, Chen J, Easterly E, Roebuck L, Ryan S, Gotwals P, et al. Blockade of TGF-beta inhibits mammary tumor cell viability, migration, and metastases. J. Clin. Invest. 2002; 109:1551–1559. [PubMed: 12070302]

Muraoka RS, Koh Y, Roebuck LR, Sanders ME, Brantley-Sieders D, Gorska AE, Moses HL, Arteaga CL. Increased Malignancy of Neu-Induced Mammary Tumors Overexpressing Active Transforming Growth Factor {beta}1. Mol. Cell. Biol. 2003; 23:8691–8703. [PubMed: 14612410]

Muraoka-Cook RS, Kurokawa H, Koh Y, Forbes JT, Roebuck LR, Barcellos-Hoff MH, Moody SE, Chodosh LA, Arteaga CL. Conditional overexpression of active transforming growth factor beta1 in vivo accelerates metastases of transgenic mammary tumors. Cancer research. 2004; 64:9002–11. [PubMed: 15604265]

Northey JJ, Chmielecki J, Ngan E, Russo C, Annis MG, Muller WJ, Siegel PM. Signaling through ShcA is required for TGF-{beta} and Neu/ErbB-2 induced breast cancer cell motility and invasion. Mol. Cell. Biol. 2008; 28:3162–76. [PubMed: 18332126]

Oakes PW, Beckham Y, Stricker J, Gardel ML. Tension is required but not sufficient for focal adhesion maturation without a stress fiber template. The Journal of cell biology. 2012; 196:363–74. [PubMed: 22291038]

Otey CA, Carpen O. Alpha-actinin revisited: a fresh look at an old player. Cell motility and the cytoskeleton. 2004; 58:104–11. [PubMed: 15083532]

Ozdamar B, Bose R, Barrios-Rodiles M, Wang HR, Zhang Y, Wrana JL. Regulation of the polarity protein Par6 by TGFbeta receptors controls epithelial cell plasticity. Science. 2005; 307:1603–9. [PubMed: 15761148]

Padua D, Massague J. Roles of TGFbeta in metastasis. Cell research. 2009; 19:89–102. [PubMed: 19050696]

Europe PMC Funders Author Manuscripts

Padua D, Zhang XH, Wang Q, Nadal C, Gerald WL, Gomis RR, Massague J. TGFbeta primes breast tumors for lung metastasis seeding through angiopoietin-like 4. Cell. 2008; 133:66–77. [PubMed: 18394990]

Petit MM, Fradelizi J, Golsteyn RM, Ayoubi TA, Menichi B, Louvard D, Van de Ven WJ, Friederich E. LPP, an actin cytoskeleton protein related to zyxin, harbors a nuclear export signal and transcriptional activation capacity. Molecular biology of the cell. 2000; 11:117–29. [PubMed: 10637295]

Petit MM, Meulemans SM, Alen P, Ayoubi TA, Jansen E, Van de Ven WJ. The tumor suppressor Scrib interacts with the zyxin-related protein LPP, which shuttles between cell adhesion sites and the nucleus. BMC Cell Biol. 2005; 6:1. [PubMed: 15649318]

Petit MM, Meulemans SM, Van de Ven WJ. The focal adhesion and nuclear targeting capacity of the LIM-containing lipoma-preferred partner (LPP) protein. J Biol Chem. 2003; 278:2157–68. [PubMed: 12441356]

Pierceall WE, Woodard AS, Morrow JS, Rimm D, Fearon ER. Frequent alterations in E-cadherin and alpha- and beta-catenin expression in human breast cancer cell lines. Oncogene. 1995; 11:1319–26. [PubMed: 7478552]

Pratt SJ, Epple H, Ward M, Feng Y, Braga VM, Longmore GD. The LIM protein Ajuba influences p130Cas localization and Rac1 activity during cell migration. The Journal of cell biology. 2005; 168:813–24. [PubMed: 15728191]

Rahimi RA, Leof EB. TGF-beta signaling: a tale of two responses. J. Cell. Biochem. 2007; 102:593–608. [PubMed: 17729308]

Safina A, Ren MQ, Vandette E, Bakin AV. TAK1 is required for TGF-beta 1-mediated regulation of matrix metalloproteinase-9 and metastasis. Oncogene. 2008; 27:1198–207. [PubMed: 17828308]

Safina A, Sotomayor P, Limoge M, Morrison C, Bakin AV. TAK1-TAB2 signaling contributes to bone destruction by breast carcinoma cells. Molecular cancer research: MCR. 2011; 9:1042–53. [PubMed: 21700681]

Safina AF, Varga AE, Bianchi A, Zheng Q, Kunnev D, Liang P, Bakin AV. Ras alters epithelial-mesenchymal transition in response to TGFbeta by reducing actin fibers and cell-matrix adhesion. Cell cycle. 2009; 8:284–98. [PubMed: 19177011]

Sen S, Dong M, Kumar S. Isoform-specific contributions of alpha-actinin to glioma cell mechanobiology. PloS one. 2009; 4:e8427. [PubMed: 20037648]

Seton-Rogers SE, Lu Y, Hines LM, Koundinya M, LaBaer J, Muthuswamy SK, Brugge JS. Cooperation of the ErbB2 receptor and transforming growth factor {beta} in induction of migration and invasion in mammary epithelial cells. Proceedings of the National Academy of Sciences. 2004; 101:1257–1262.

Siegel PM, Shu W, Cardiff RD, Muller WJ, Massague J. Transforming growth factor {beta} signaling impairs Neu-induced mammary tumorigenesis while promoting pulmonary metastasis. Proceedings of the National Academy of Sciences. 2003; 100:8430–8435.

Sjoblom B, Salmazo A, Djinovic-Carugo K. Alpha-actinin structure and regulation. Cellular and molecular life sciences: CMLS. 2008; 65:2688–701. [PubMed: 18488141]

Thiery JP, Acloque H, Huang RY, Nieto MA. Epithelial-mesenchymal transitions in development and disease. Cell. 2009; 139:871–90. [PubMed: 19945376]

Tomaskovic-Crook E, Thompson EW, Thiery JP. Epithelial to mesenchymal transition and breast cancer. Breast cancer research: BCR. 2009; 11:213. [PubMed: 19909494]

Ueda Y, Wang S, Dumont N, Yi JY, Koh Y, Arteaga CL. Overexpression of HER2 (erbB2) in human breast epithelial cells unmasks transforming growth factor beta-induced cell motility. The Journal of biological chemistry. 2004; 279:24505–13. [PubMed: 15044465]

Uemura A, Nguyen TN, Steele AN, Yamada S. The LIM domain of zyxin is sufficient for force-induced accumulation of zyxin during cell migration. Biophysical journal. 2011; 101:1069–75. [PubMed: 21889443]

Ursini-Siegel J, Hardy WR, Zuo D, Lam SHL, Sanguin-Gendreau V, Cardiff RD, Pawson T, Muller WJ. ShcA signalling is essential for tumour progression in mouse models of human breast cancer. EMBO. 2008; 27:910–920.

Vervenne HB, Crombez KR, Delvaux EL, Janssens V, Van de Ven WJ, Petit MM. Targeted disruption of the mouse Lipoma Preferred Partner gene. Biochem Biophys Res Commun. 2009; 379:368–73. [PubMed: 19111675]

Vervenne HB, Crombez KR, Lambaerts K, Carvalho L, Koppen M, Heisenberg CP, Van de Ven WJ, Petit MM. Lpp is involved in Wnt/PCP signaling and acts together with Scrib to mediate convergence and extension movements during zebrafish gastrulation. Dev Biol. 2008; 320:267–77. [PubMed: 18582857]

Vicente-Manzanares M, Choi CK, Horwitz AR. Integrins in cell migration--the actin connection. J Cell Sci. 2009; 122:199–206. [PubMed: 19118212]

Viloria-Petit AM, David L, Jia JY, Erdemir T, Bane AL, Pinnaduwage D, Roncari L, Narimatsu M, Bose R, Moffat J, et al. A role for the TGFbeta-Par6 polarity pathway in breast cancer progression. Proceedings of the National Academy of Sciences of the United States of America. 2009; 106:14028–33. [PubMed: 19667198]

Wang SE, Shin I, Wu FY, Friedman DB, Arteaga CL. HER2/Neu (ErbB2) signaling to Rac1-Pak1 is temporally and spatially modulated by transforming growth factor beta. Cancer research. 2006; 66:9591–600. [PubMed: 17018616]

Wang SE, Xiang B, Guix M, Olivares MG, Parker J, Chung CH, Pandiella A, Arteaga CL. Transforming growth factor beta engages TACE and ErbB3 to activate phosphatidylinositol-3 kinase/Akt in ErbB2-overexpressing breast cancer and desensitizes cells to trastuzumab. Molecular and cellular biology. 2008; 28:5605–20. [PubMed: 18625725]

Wang SE, Xiang B, Zent R, Quaranta V, Pozzi A, Arteaga CL. Transforming growth factor beta induces clustering of HER2 and integrins by activating Src-focal adhesion kinase and receptor association to the cytoskeleton. Cancer research. 2009; 69:475–82. [PubMed: 19147560]

Wendt MK, Smith JA, Schiemann WP. Transforming growth factor-beta-induced epithelial-mesenchymal transition facilitates epidermal growth factor-dependent breast cancer progression. Oncogene. 2010; 29:6485–98. [PubMed: 20802523]

Wiercinska E, Naber HP, Pardali E, van der Pluijm G, van Dam H, ten Dijke P. The TGF-beta/Smad pathway induces breast cancer cell invasion through the up-regulation of matrix metalloproteinase 2 and 9 in a spheroid invasion model system. Breast cancer research and treatment. 2011; 128:657–66. [PubMed: 20821046]

Wilkes MC, Leof EB. Transforming growth factor beta activation of c-Abl is independent of receptor internalization and regulated by phosphatidylinositol 3-kinase and PAK2 in mesenchymal cultures. The Journal of biological chemistry. 2006; 281:27846–54. [PubMed: 16867995]

Willier S, Butt E, Richter GH, Burdach S, Grunewald TG. Defining the role of TRIP6 in cell physiology and cancer. Biology of the cell / under the auspices of the European Cell Biology Organization. 2011; 103:573–91. [PubMed: 22054418]

Wolfenson H, Bershadsky A, Henis YI, Geiger B. Actomyosin-generated tension controls the molecular kinetics of focal adhesions. Journal of cell science. 2011; 124:1425–32. [PubMed: 21486952]

Xu J, Lamouille S, Derynck R. TGF-beta-induced epithelial to mesenchymal transition. Cell research. 2009; 19:156–72. [PubMed: 19153598]

Yi J, Beckerle MC. The human TRIP6 gene encodes a LIM domain protein and maps to chromosome 7q22, a region associated with tumorigenesis. Genomics. 1998; 49:314–6. [PubMed: 9598321]

Yin JJ, Selander K, Chirgwin JM, Dallas M, Grubbs BG, Wieser R, Massague J, Mundy GR, Guise TA. TGF-beta signaling blockade inhibits PTHrP secretion by breast cancer cells and bone metastases development. The Journal of clinical investigation. 1999; 103:197–206. [PubMed: 9916131]

Zhang H, Chen X, Bollag WB, Bollag RJ, Sheehan DJ, Chew CS. Lasp1 gene disruption is linked to enhanced cell migration and tumor formation. Physiol Genomics. 2009; 38:372–85. [PubMed: 19531578]

Zhang L, Wang W, Hayashi Y, Jester JV, Birk DE, Gao M, Liu CY, Kao WW, Karin M, Xia Y. A role for MEK kinase 1 in TGF-beta/activin-induced epithelium movement and embryonic eyelid closure. The EMBO journal. 2003; 22:4443–54. [PubMed: 12941696]

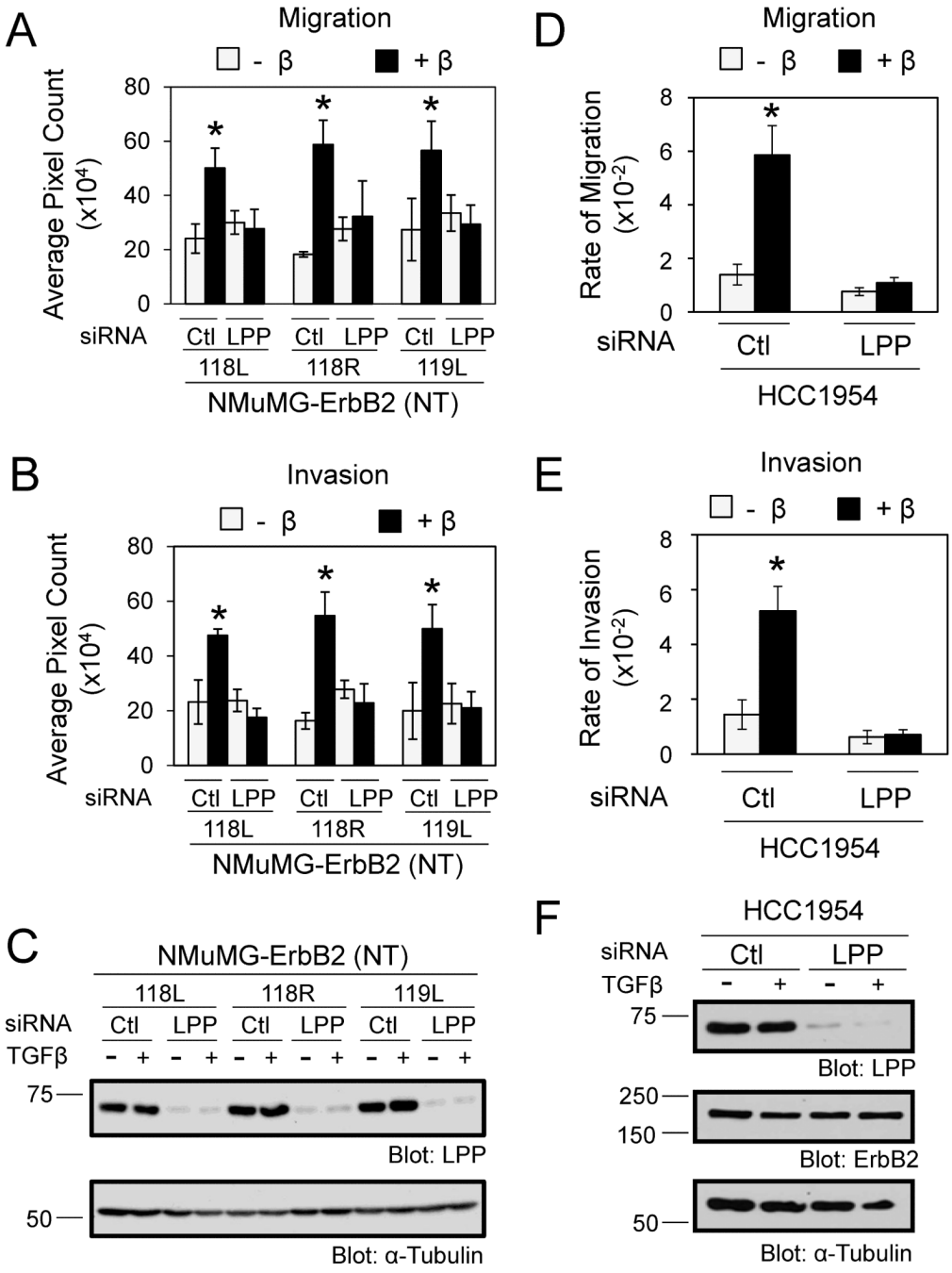

Figure 1. LPP is required for TGFβ-induced migration and invasion of ErbB2-expresing breast cancer cells that undergo an EMT

Three independent NMuMG-ErbB2 explants (indicated by number/letter designations: 118L, 118R and 119L) were transfected with control (Ctl) or LPP-targeting siRNAs (LPP) and incubated with or without TGFβ for 24 hours prior to plating into Boyden chambers. (A, B) Cells that have migrated or invaded to the underside of the transwell were fixed and stained. Data represents 3 independent experiments performed in duplicate. (C) Total cell lysates were collected at the endpoint of the assays and immunoblotted for LPP, with α-Tubulin serving as a loading control. HCC1954 human breast tumor cells were transfected with control (Ctl) or LPP targeting siRNAs (LPP). (D, E) The rate of cell migration and

invasion of untreated or TGFβ stimulated cells were assessed by xCELLigence system. Data represents 3 independent experiments performed in duplicate. (F) Total cell lysates were collected at assay endpoint and immunoblotted for LPP, ErbB2 and α-Tubulin. TGFβ induces significant increases in cell migration (A; *, $P < 0.002$, D; *, $P = 0.008$) and invasion (B; *, $P < 0.001$, E; *, $P = 0.007$) in 2 independent mammary tumor cell systems, and this response is abolished in the absence of LPP.

Europe PMC Funders Author Manuscripts

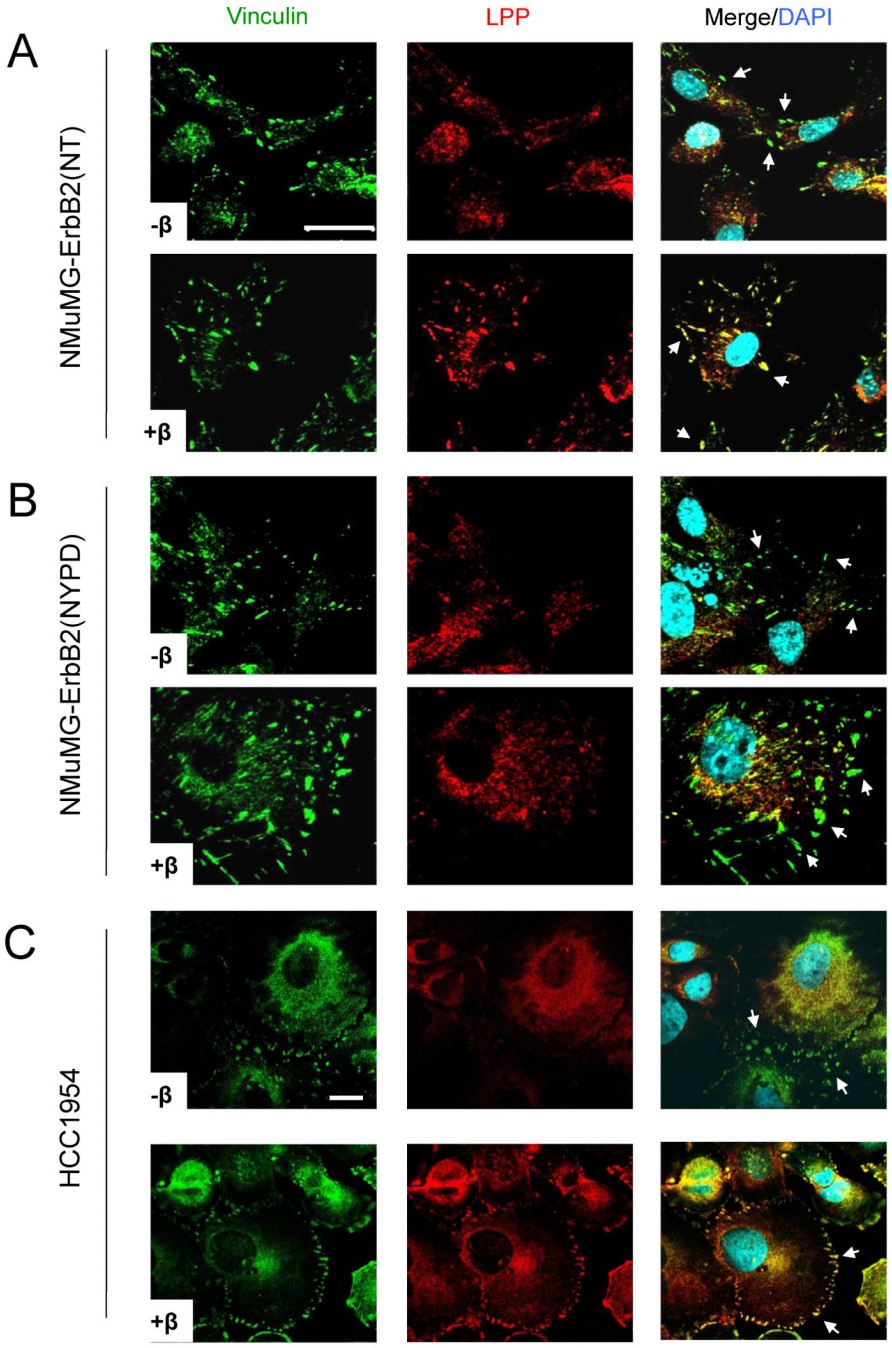

Figure 2. LPP co-localizes to focal adhesions in response to TGFβ stimulation

(A-C) NMuMG-ErbB2(NT), NMuMG-ErbB2(NYPD) and HCC1954 cells were plated onto glass coverslips and treated with or without TGFβ for 24 hours. A wound was made in each monolayer and cells were cultured for an additional 6 hours. Cells were then fixed and stained with antibodies directed against LPP and Vinculin, followed by Alexa Fluor dye conjugated secondary antibodies. DAPI was used to stain the nucleus. Representative images are shown. White arrows point to focal adhesions. (Scale bar: A and B = 20 μm; C = 20 μm).

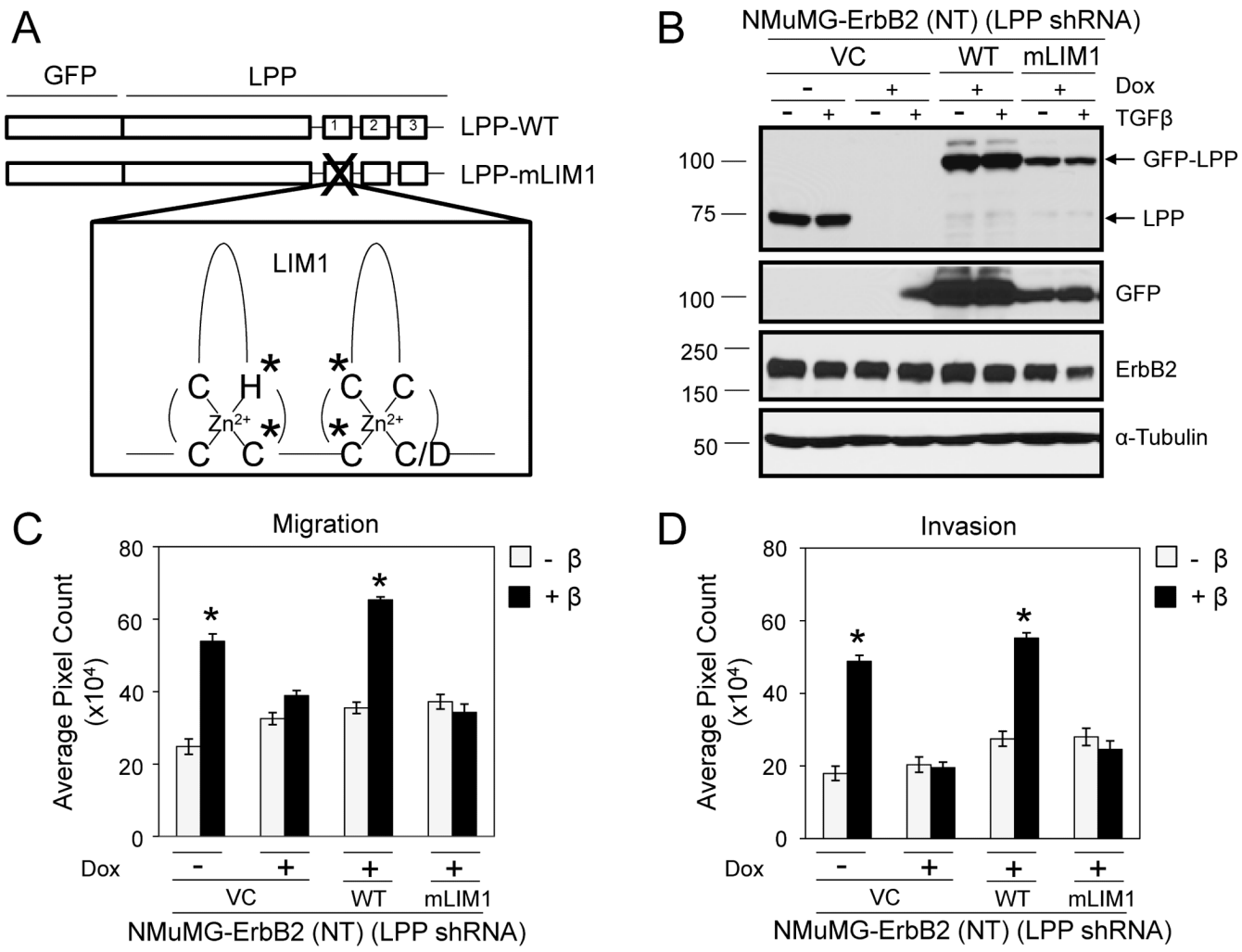

Figure 3. LPP targeting to focal adhesions is critical for TGFβ-induced migration and invasion of ErbB2-expresing breast cancer cells

(A) Schematic diagram of GFP-tagged LPP wild-type (LPP-WT) construct and GFP-tagged LPP construct harbouring mutations to the LIM1 domain (LPP-mLIM1). Amino acid residues marked with (*) were substituted to Alanine. (B) Immunoblot analyses of NMuMG-ErbB2 cells expressing a dox-inducible shRNA against the 3′UTR of LPP, in which an empty vector (VC), EGFP tagged wild-type LPP (WT) or EGFP tagged LIM1 mutant LPP (mLIM1) are also expressed. Cells were stimulated with or without doxycycline and TGFβ as indicated. Antibodies against LPP and GFP were used to detect the presence of endogenous or exogenous LPP, respectively. ErbB2 levels remain unchanged and α-Tubulin was used as a loading control. (C, D) NMuMG-ErbB2 cell populations treated with or without doxycycline and TGFβ were subjected to migration and invasion assays using Boyden chambers. Cells were stained and fixed after 24 hours and 5 images were captured from the underside of each transwell. The data is expressed as the average pixel count obtained from 3 independent experiments performed in duplicate (*; $P < 0.001$).

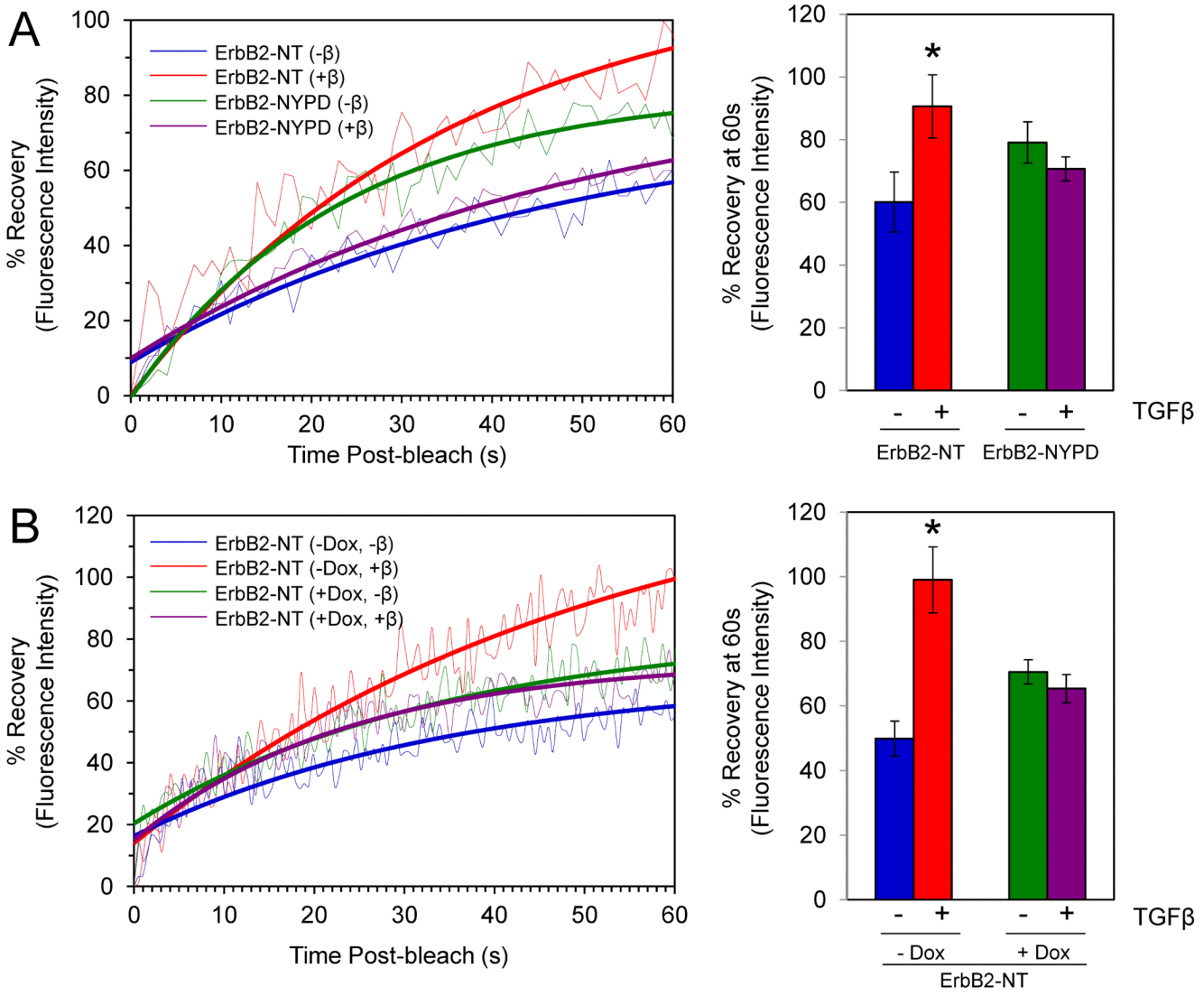

Figure 4. LPP promotes focal adhesion turnover

(A) NMuMG-ErbB2 NT and NYPD cells were transfected with Paxillin-GFP and plated onto glass bottom culture dishes coated with fibronectin. Cells were stimulated with or without TGFβ for 24 hours prior to Fluorescence Recovery after Photo-bleaching (FRAP) analysis. The raw traces and fitted exponential recovery curves are shown and represent the average of 12-19 adhesions at the leading edge from each cell population. The final % recovery at 60s is also plotted (NT-β: 60.1 ± 9.6%, NT+β: 90.6 ± 10.1%, NYPD-β: 79.1 ± 6.6%, NYPD+β: 70.7 ± 3.8%). *; $P < 0.040$. (B) NMuMG-ErbB2-NT cells expressing a LPP targeting shRNA under the control of a dox-inducible system were stimulated with or without doxycycline for 72 hours prior to being transfected with paxillin-GFP. Cells were plated onto glass bottom dishes coated with fibronectin and stimulated with or without TGFβ for 24 hours and then subjected to FRAP analysis. The raw traces and fitted exponential recovery curves are shown and represent the average of 18-28 adhesions from each cell population. The final % recovery at 60s is plotted (−Dox, −β: 49.8 ± 5.4%; −Dox +β: 98.9 ± 10.2%; +Dox, −β: 70.5 ± 3.7%; +Dox, +β: 65.3 ± 4.4%). *; $P < 0.001$.

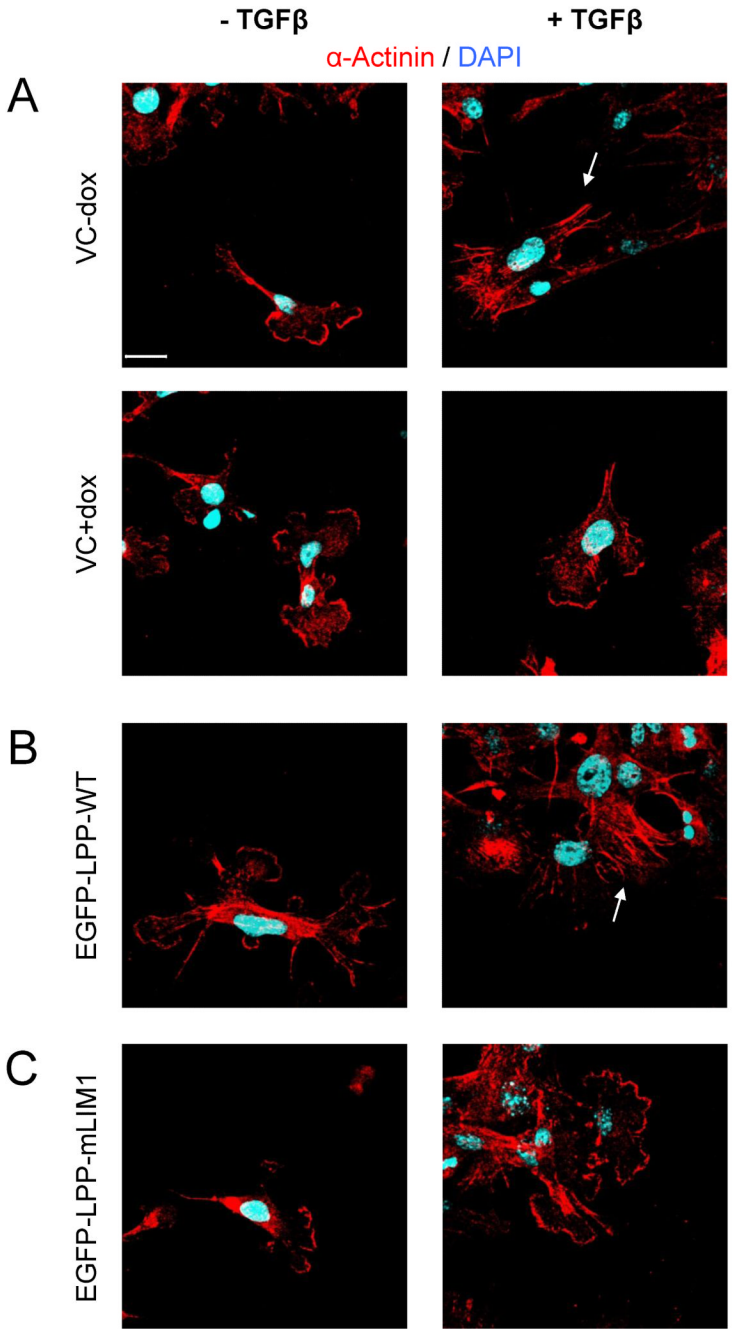

Figure 5. α-Actinin fails to localize to actin stress fibers when LPP cannot be targeted to focal adhesions

(A-C) NMuMG-ErbB2 cells expressing a dox-inducible shRNA against the 3′UTR of LPP and an empty vector (VC), LPP-WT or LPP-mLIM1were stimulated with or without doxycycline prior to plating onto glass coverslips. Cells were then stimulated with or without TGFβ for 24 hours. A wound was made in the monolayer and cells were cultured for an additional 6 hours. Cells were fixed and stained with an α-Actinin specific antibody followed by incubation with an Alexa Fluor 555nm conjugated secondary antibody. DAPI was used to stain the nucleus. White arrows indicate stress fibers. Representative images are shown (Scale bar = 20μm for all images).

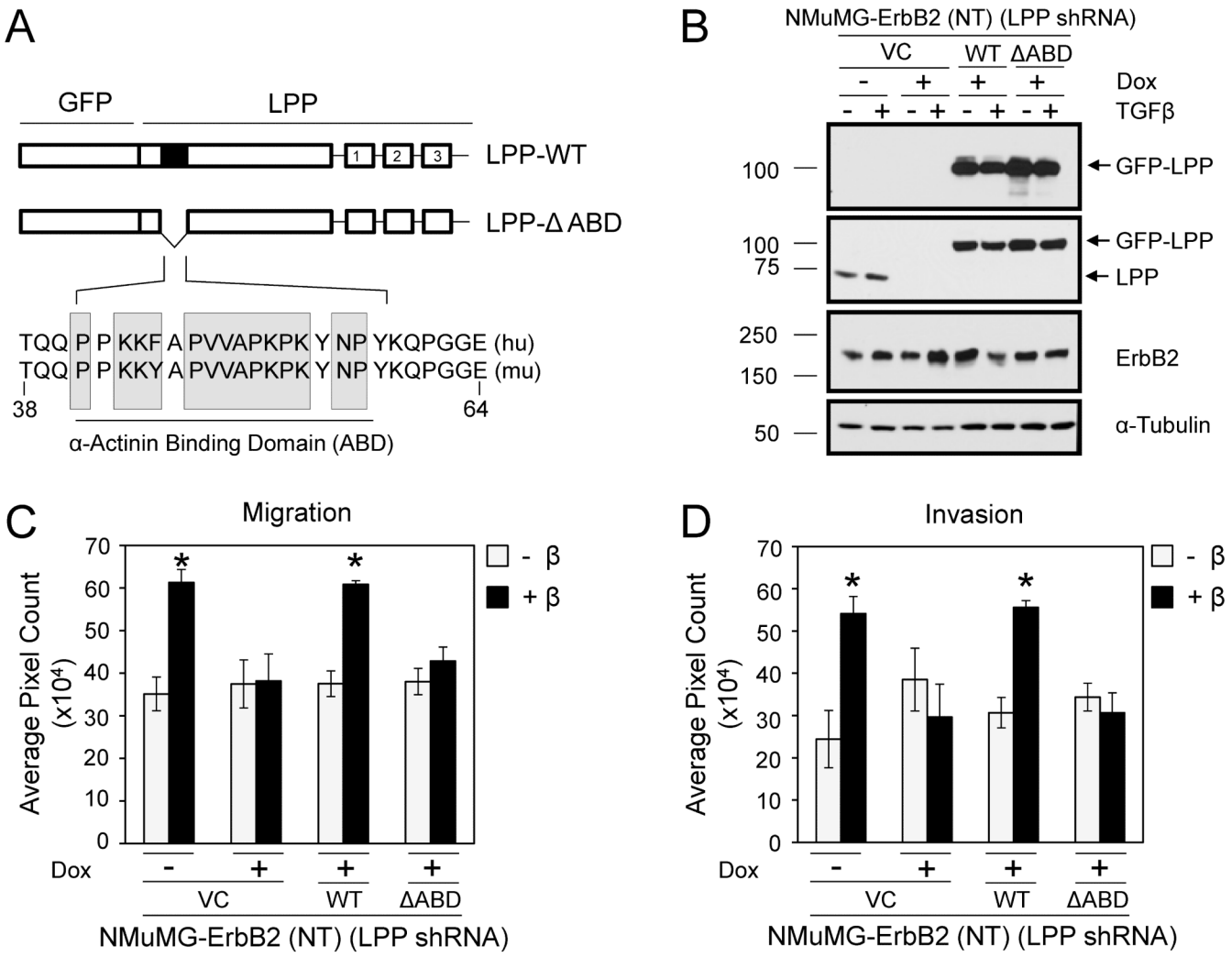

Figure 6. An LPP mutant that cannot bind α-Actinin fails to rescue TGFβ-induced migration and invasion of ErbB2-expressing cells

(A) Schematic diagram of GFP-tagged LPP wild-type (LPP-WT) construct and a GFP-tagged LPP construct harbouring a deletion in its α-Actinin binding domain (LPP-ΔABD). The amino acids removed by the deletion are indicated. (B) Immunoblot analyses of NMuMG-ErbB2 cells expressing a dox-inducible shRNA against the 3′UTR of LPP, in which an empty vector (VC), EGFP-LPP-WT or EGFP-LPP-ΔABD are expressed. Cells were stimulated with or without doxycycline and TGFβ as indicated. Antibodies against LPP and GFP were used to detect the presence of endogenous or exogenous LPP respectively. ErbB2 levels remain unchanged and α-Tubulin was used as a loading control. (C, D) NMuMG-ErbB2 cell populations treated with or without doxycycline and TGFβ were subjected to migration and invasion assays. The data is expressed as the average pixel count obtained from 3 independent experiments performed in duplicate (*; $P < 0.005$).

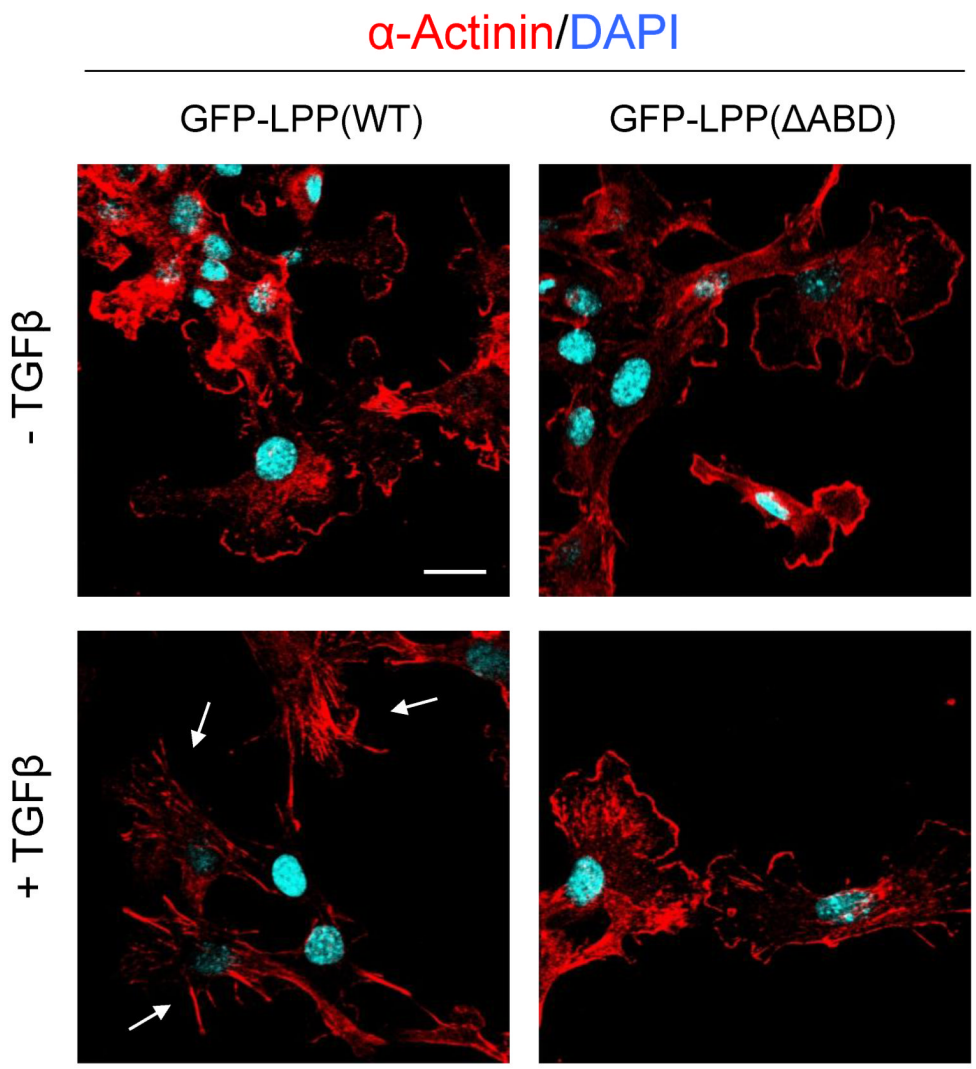

Figure 7. α-Actinin fails to localize with stress fibers following TGFβ stimulation in cells expressing GFP-LPP(ΔABD)

Cells harboring EGFP-LPP(WT) and EGFP-LPP(ΔABD) were treated with doxycycline and plated onto glass coverslips prior to stimulation with or without TGFβ for 24 hours. A wound was made in the monolayer and cells were cultured for an additional 6 hours. Cells were then fixed and stained with an antibody directed against α-Actinin, followed by Alexa Fluor 555nm dye conjugated secondary antibody. DAPI was used to stain the nucleus. White arrows indicate stress fibers. Representative images are shown (scale bar = 20μm for all images).

Table 1

LPP colocalization to Focal Adhesions in response to TGFβ stimulation in ErbB2-expressing breast cancer cells

NMuMG Explant		% of Adhesions with LPP[a]	*p* values	Average $I_{LPP}/I_{vinculin}$ Ratio in LPP-Positive Adhesions[b]	*p* values
ErbB2 (NT)	−TGFß +TGFß	69.4 ± 7.8 94.8 ± 12.9	0.019	0.64 ± 0.09 1.17 ± 0.16	0.012
ErbB2 (NYPD)	−TGFß +TGFß	82.1 ± 12.3 65.7 ± 5.6	0.25	0.58 ± 0.12 0.73 ± 0.07	0.3
Cell Line		**% of Adhesions with LPP[a]**	***p* values**	**Average $I_{Lpp}/I_{vinculin}$ Ratio in LPP-Positive Adhesions[b]**	***p* values**
HCC 1954	−TGFß +TGFß	68.6 ± 9.5 95.0 ± 1.9	0.032	0.51 ± 0.16 1.16 ± 0.11	0.005

[a]The percentage colocalization of LPP and Vinculin was calculated by creating a binary mask of Vinculin-positive adhesions using Integrated Morphometry Analysis. The mask was then applied to determine the number of Vinculin adhesions that also contain LPP-positive staining.

[b]The signal intensity of LPP relative to Vinculin was calculated by isolating LPP adhesions that colocalized to Vinculin adhesions. The average total intensity of LPP and Vinculin adhesions was measured. The Intensity Ratio was obtained by dividing the average total intensity of LPP adhesions by the average total intensity of Vinculin adhesions.

The total number of objects quantified for each cell line is as follows: NT - ß = 1170, NT + ß = 1440, NYPD - ß = 1505, NYPD + ß = 1625, HCC1954 - ß = 2139, HCC1954 + ß = 3671.